TU Delft

Delft University of Technology

Assembly of shells with bi-stable mechanism

Chiang, Y.-C.; Mostafavi, Sina; Bier, Henriette

Publication date
2018

Document Version
Final published version

Published in
Proceedings of Advances in Architectural Geometry 2018 (AAG 2018)

Citation (APA)
Chiang, Y.-C., Mostafavi, S., & Bier, H. (2018). Assembly of shells with bi-stable mechanism. In L. Hesselgren, A. Kilian, S. Malek, K.-G. Olsson, O. Sorkine-Hornung, & C. Williams (Eds.), *Proceedings of Advances in Architectural Geometry 2018 (AAG 2018)* (pp. 54-71). Chalmers University of Technology.

Important note
To cite this publication, please use the final published version (if applicable).
Please check the document version above.

Copyright
Other than for strictly personal use, it is not permitted to download, forward or distribute the text or part of it, without the consent of the author(s) and/or copyright holder(s), unless the work is under an open content license such as Creative Commons.

Takedown policy
Please contact us and provide details if you believe this document breaches copyrights.
We will remove access to the work immediately and investigate your claim.

This work is downloaded from Delft University of Technology.
For technical reasons the number of authors shown on this cover page is limited to a maximum of 10.

AAG2018

Advances in Architectural Geometry 2018

Lars Hesselgren, Axel Kilian, Samar Malek
Karl-Gunnar Olsson, Olga Sorkine-Hornung
Chris Williams
Editors

CHALMERS

All rights reserved. Nothing from this publication may be reproduced, or published in any form or in any manner, including electronic, mechanical, reprographic or photographic, without prior written permission from the publisher or the author.

© 2018, Chalmers University of Technology, Department of Architecture and Civil Engineering

Printed in Vienna 2018
Published by Klein Publishing GmbH (Ltd.)
kpv@gmx.at
ISBN 978-3-903015-13-5

Download open access:
https://research.chalmers.se/en/publication/504188
www.chalmers.se
info@chalmers.se

Cover illustration by Goswin Rothenthal, Djordje Spasic and René Ziegler, Waagner-Biro Stahlbau AG; Ateliers Jean Nouvel, architect and TDIC owner, “Oasis of Light – Dome – Outer Cladding”

Host:
CHALMERS

Supported by:
City of Gothenburg

Gold sponsor:
wsp

Silver sponsor:
AUTODESK.

Bronze sponsors:
waagner biro
white
Semrén+Månsson
Johanneberg Science Park
KUKA
FOJAB arkitekter
SWECO

Assembly of shells with bi-stable mechanism

Yu-Chou Chiang, Sina Mostafavi, Henriette Bier

Yu-Chou Chiang
Chiang.YuChou@gmail.com
Robotic Building, Delft University of Technology, Netherlands

Sina Mostafavi
S.Mostafavi@tudelft.nl
Robotic Building, Delft University of Technology, Netherlands

Henriette Bier
H.H.Bier@tudelft.nl
Robotic Building, Delft University of Technology, Netherlands

Keywords:
Bi-stable mechanism, reconfigurable assembly, shell structure, free-form construction, programmable material

Abstract

Shell structures achieve stability through double curvature, which brings about construction challenges. This paper presents a strategy to design and assemble a panelized shell with a bi-stable mechanism aiming to make the assembly process more efficient. The developed prototype has two states of flat and three-dimensional stable configuration. This reconfiguration is achieved by reconfiguring the flattened surface of a shell into a three-dimensional structure using embedded bi-stable joints. In order to apply this approach on free-form double curved shells, a workflow to translate a shell into its flattened state is developed. Discrete components are connected using bi-stable joints, where each joint has two stable states. Once the joints are mechanically activated, they guide the adjacent components contracting and rotating into the three-dimensional configuration. Initial explorations indicate that an edge of a shell will turn into an isosceles trapezoid in the flattened configuration while a node of a conical mesh will turn into a cyclic quadrilateral in the flattened configuration. The flattening process is demonstrated using a free-form vault, while scaled physical porotypes are 3D printed with PLA and tested. Future studies require exploration into applications with construction materials at larger scales.

1. Introduction

Double curved surfaces give shell structures their structural integrity and architectural expression, while being at the same time challenging with respect to construction. Between the 1920s and 1960s, numerous site-cast concrete thin-shells were built, then, because the geometry was confined to regular forms (e.g., sphere and paraboloids) and it required labor-intensive formwork, the construction of concrete shell declined (Meyer & Sheer 2005). Since the 2000s, with the increasing demand on free-form architectures, thin-shell structures in the forms of grid-shells and tessellated roofs have attracted the attention of architects, engineers, and geometricians (Pottmann et al. 2015).

Today, several technologies facilitate the revival of the thin-shell structure, including structural form-finding algorithms, numerical geometry optimization, and computational controlled machinery (Van Mele et al. 2016). By applying these methods, production of the geometrically

complex components becomes manufacturable within a moderate budget. However, assembly remains labor-intensive work. Both formworks for cast-in-place concrete and falseworks for on-site assembly demand considerable labor to assemble. To improve the assembly process, it is necessary to explore methods addressing this problem.

This research introduces an alternative way of assembling shell structures. The goal is to develop a methodology to decompose a shell structure into panels connected by bi-stable joints in a flat configuration. Then, through reconfiguration, the bi-stable joint will guide adjacent panels contracting and rotating into the pre-programmed position. As a visualized example, Figure 1 shows the overall process of translation and reconfiguration from flat to double-curved of a dome-like shell.

In this paper, the focus is on the geometrical aspect of the bi-stable mechanism. Further material tests, actuating strategy, static and dynamic analysis will be explored at building scale.

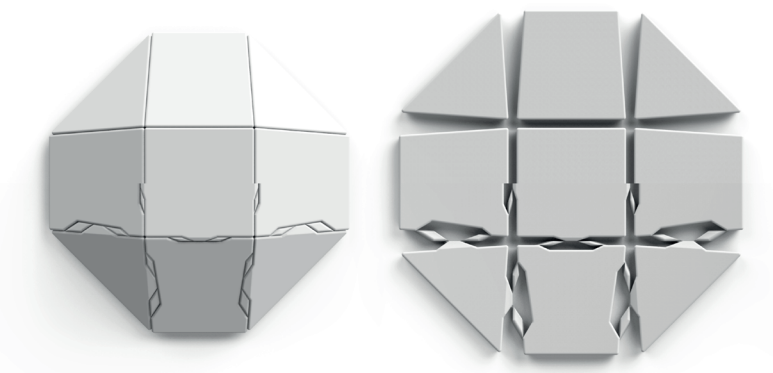

Figure 1: Top views of a dome are showcasing the four phases of the proposed workflow. The workflow starts from a panelized shell (top left), followed by its flattened configuration (top right) and the installation of bi-stable joints (bottom right). Once the assemblage is mechanically activated, it turns to the completed assembly (bottom left).

1.1 Outline

Related assembly approaches and the development of reconfigurable bi-stable mechanisms are introduced in the background section. Then, in the methods section, mechanical and geometrical details of the established bi-stable mechanism are presented. A novel bi-stable mechanism

capable of out-of-plane rotation is proposed. The criteria for unrolling a shell into its flattened state are identified. Some physical prototypes applying these methods are shown in the result section. In conclusion, the findings are summarized, and the future research is proposed.

2. Background

In order to enhance the stagnating productivity in the architecture, engineering and construction sector (McKinsey Global Institute, 2017), assembly, especially on-site assembly, need to take advantage of automation.

From a holistic view, assembly (or assembly-aware design) is not merely combing separate components together; it is a constructional strategy to discretize an assemblage into manufacturable components then aggregate the components into the completed assemblage. There are numerous research projects investigating the interrelation between design and assembly. By identifying the difference between the various schemes, an interesting approach to carry out assembly stood out, reconfigurable assembly.

Reconfigurable assembly could be defined as a constructional strategy to aggregate components in a simple and manufacturable configuration, and then reconfigure the assemblage into the desired complex configuration. For instance, A 3D-printed straight line can be reconfigured into a wavy curve or a set of polygons on a flat plan can be reconfigured into a polyhedron (Tibbits, McKnelly, Olguin, Dikovsky, & Hirsch, 2014; van Manen, Janbaz, & Zadpoor, 2017). Potentially, the reconfigurable mechanisms can reduce the number of independent components in a system (Tibbits et al., 2014); an object can be stored and transported in the compact configuration, then be deployed to the serving configuration (Haghpanah, Salari-Sharif, Pourrajab, Hopkins, & Valdevit, 2016).

The previous published shape-reconfigurable mechanisms are achieved through expanding, contracting materials or architected materials. The first approach mainly relies on special materials that are capable of expanding or contracting when the environment is changing. For example, a folding mechanism can be created by layering two materials, which have different expansion rate in water, ensuring that a box can be reconfigured from a flat 3D-printed object (Tibbits et al., 2014). This type

of approach requires a special expanding material and the corresponding environmental change to activate the expansion

The other approach involves designed porosity within the constituent material, and such porosity makes the material bendable and stretchable, which are termed as architected shape-reconfigurable materials (Konaković et al., 2016; Rafsanjani & Pasini, 2016). Inspired by the research of "Beyond Developable" (Konaković et al., 2016), where researchers developed algorithms to translate a flat auxetic material to a double curved surface. The stretchable mechanisms open up an insight of how to approximate a double curved surface. To be noted that, this auxetic mechanism has a certain flexibility, therefore, it is vulnerable to deform when external forces are applied.

Conversely, there is a type of architected materials can stably maintain it reconfigured shape, termed bi-stable or multi-stable mechanisms (Haghpanah et al., 2016; Rafsanjani & Pasini, 2016). It provides an interesting reconfiguration feature: the scale factor between the two stable states can be engineered, and the two stable states have the mechanical strength to resist external forces. However, for the time being, the published bi-stable mechanisms are limited to in-plane or two dimensional reconfigurations.

Inspired by the development of the auxetic mechanism and the bi-stable mechanisms, this research investigates the application of bi-stable auxetic mechanisms in flat-to-curved reconfigurable shell structures.

3. Methods

In the method section, three aspects of the workflow are discussed. Considering the overview of the processes introduced in Figure 1, illustrating the panelization of a shell, this section addresses the methods with emphasis on the technical details of the bi-stable mechanism. In the first sub-section, the basic in-plan translation of the bi-stable mechanism is presented. Then, geometric features of the proposed out-of-plane rotation of bi-stable mechanism are introduced. The third sub-section discusses the panelization process for flattening a double-curved surface. By applying these processes, a given double curved shell can be flattened into a bi-stable reconfiguring mechanism.

3.1 Mechanical features of the in-plane translation of bi-stable mechanisms

A basic bi-stable mechanism is represented by a unit where two beams are connected by a hinge and binned at two supports (Haghpanah et al., 2016; Huang & Vahidi, 1971). The idealized structure unit is depicted in Figure 2 (top). When the unit is subjected to an external force at the center of the hinge, the two inclined beams compress against each other. More specifically, the external force is balanced by the vertical components of the axial compressions of the two inclined beams. The axial compressions make the beams shortened, resulting in the downward displacement of the center hinge. In the case that the external force is small and removed afterward, the beams will spring back to the original state, noted as the first stable state in Figure 2. In a case that the external force makes the axial forces of the beams either reach the Euler buckling critical load or the beams are too flat to provide effective vertical components, the mechanism arrives its critical state and consequently, it snaps-through. After the external force is removed, and all the material spring back to its original length, the mechanism rests in the alternative configuration, noted as the second stable state in Figure 2. Although the mechanical deformation of the material does happen during the reconfiguration, geometrically, the two stable states can be simply regarded as two possible solutions of the circle-circle intersection.

The load-displacement response of the mechanism in two scenarios is illustrated in Figure 2. Cases with different beam thickness are presented. The red case has thicker beams, reconfigures without Euler buckling and it has a smooth load-displacement response curve, indicated in red in the diagram. The blue case with thinner beams has a higher tendency of buckling. The sharp turns in the blue curve indicate the start and the end of buckling. The critical states of the two cases are indicated with the circles in the diagram. It is noteworthy that the critical state of the blue case is reached easier than the other, because of the Euler buckling; less force or less displacement is required.

In the reconfiguration, two features are important for the application. First, the critical force can be programmed with tuning the stiffness of the inclined beams. Secondly, the displacement is controlled by the following formula:

$$\delta = 2 \cdot L \cdot \sin \alpha \tag{1}$$

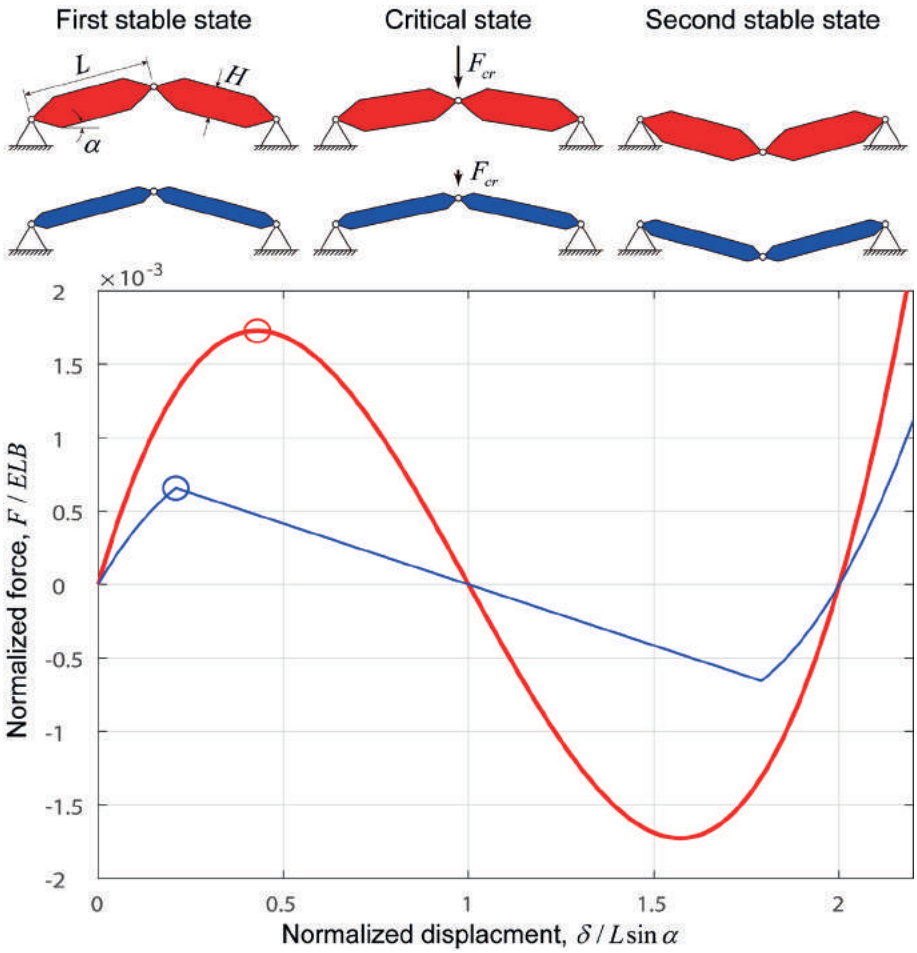

Figure 2: Basic bi-stable mechanisms and their load-displacement response: The first and second stable states have normalized displacement of 0 and 2 respectively. The critical states are indicated with the circles. E elastic modular of the material, B width of the beam, δ displacement of the center hinge.

The displacement formula can be applied to create a difference of displacements on top and bottom surface to create a bending mechanism. For more detail, the geometrical features of such mechanism are explored and discussed in the following sub-section.

3.2 Geometric features of the basic and proposed bi-stable joints

The previously published projects on bi-stable joints mainly focus on in-plane or two-dimensional translations. To create a bi-stable mecha-

nism capable of out-of-plane bending and bring adjacent panels together, further adaptation and exploration are necessary. Starting from the basic unit mentioned in the previous sub-section, the inclined beams are turned into a pair of the bi-stable connector to link two panels. One of the panels is connected to the center hinge, and the other one to the supports. Subsequently, the parallel contraction is achieved on condition that the lengths of the two connectors at the top and bottom surface are the same. An example of panels linked by a pair of connectors is shown in Figure 3a. When a connector has a shorter length than the other, an in-plane rotation can be achieved (**Fig. 3b**). In order to trigger a reconfiguration and make the mechanism allow for bending, the displacements at the top and bottom surface should be different. The contracting displacement, as shown in Equation (1), is related to rotating angle and length of the rotating arm. To avoid torsion, the rotating angle shall remain constant in a single object. Conversely, it is possible to enlarge or shorten the rotating arms. In Figure 3c, the rotating arms at the top surface (i.e. L_{aT} and L_{aB}) are smaller than the counterparts at the bottom. Subsequently, the bending is achieved. After the two bi-stable connectors with different distances of contraction are created, an in-plane rotation can also be integrated (**Fig. 3d**).

To be noted that, during the reconfiguration, each element rotates around its axis, and undergoes a temporary deformation as suggested in the previous sub-section. When the elements spring back to their original length, the system reaches the second stable state. Figure 4 shows the rotation of each element relative to the panel in the back (gray). During the reconfiguration, the red and blue connectors rotate around the physical hinges (the dash-dotted axes in red and blue). Meanwhile, the green panels rotate around the green axis.

In addition to the orientation of the axes and the hinges, the contact surfaces between the elements need to be designed. Considering the fact that the axes line of the hinges (red and blue colors) have to have a point intersection with the rotation axis line of the panels (green color), a mapping method is proposed to transform a lateral surface of a cone around the rotation axis to a rectangle (**Fig. 5**). On the rectangular image, it is possible to design various patterns then translate the pattern to physical cases. One of the pattern and the result is shown in Figure 5. As a constraint, the void space between the two panels has to be an isosceles trapezoid.

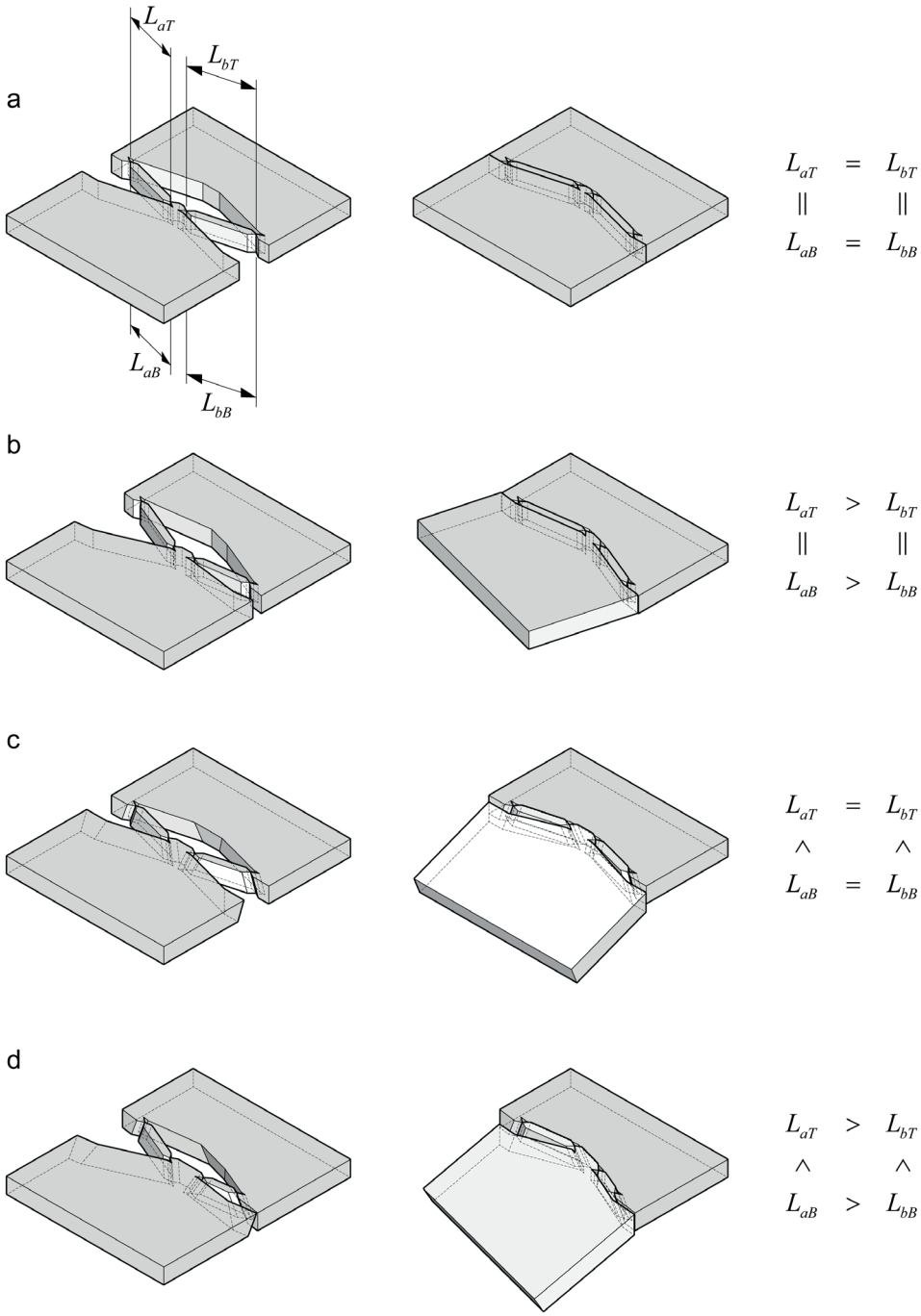

Figure 3: Joints with different degrees-of-freedom. Flattened states and curved states are shown in the left and middle column respectively. The different arrangements of the rotating arm (right column) can result in different degrees-of-freedom in the reconfiguration.

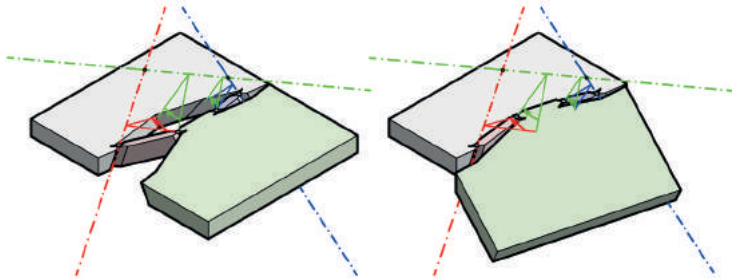

Figure 4: The geometric detail of the reconfiguring process: The flattened stable state (left) can be reconfigured into the curved stable state (right). The dash-dotted lines indicate the rotation axes; the colored arrowheads suggest the rotating directions of the corresponding elements.

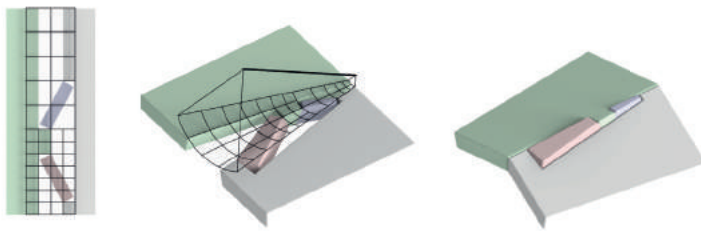

Figure 5: The conformal mapping grids show how to transform the design pattern on the rectangular(left) to the conical surface (middle). The reconfigured result is shown on the right.

This sub-section described the process of transforming an edge connected to two panels to the flattened configuration with the bi-stable mechanism. Two features affect the following process. These features are results of the adjacent panels rotating around the same axes. First, the rotation axis must be located on the bisector planes of the angle between the two panels (in the curved state). Secondly, the void between the panels in the flattened state has to be an isosceles trapezoid. In the next subsection the unrolling of a shell to a flattened configuration, with integrated reconfigurable joints is explained.

3.3 Panelization and unrolling of a panelized shell into the flattened state

As mentioned, the rotation axis has to be in the bisector plane of the dihedral angle between adjacent panels. Furthermore, the rotation axis dictates the orientation of the hinges and the interface between panels and connectors. For a node, each surrounding edge introduces one in-

terface with such orientation. One may prefer all the interfaces intersect each other at the same axis. In such case, one of the findings of the research is that the co-axis of every node dictates the tessellation to be conical meshes (Liu, Pottmann, Wallner, Yang, &Wang, 2006).

The constraint of the isosceles trapezoid and the preference of the conical mesh determine that a node has to be a cyclic polygon in the flattened state as shown in Figure 6. The panels are shaded in gray, and the symmetric axis of the trapezoid illustrated in dash-dotted lines. The proving of the cyclic quadrilateral is separated in two parts.

The first part of the proving explains that, in the flattened state, the vertex of a panel (**Fig. 6**) have to be on an arc if the two neighbor panels are fixed. Considering a node surrounded by four panels, in a flattened state, and the location of the second panel (P_2) is not determined yet while the other P_1 and P_3 are fixed. By the round angle around

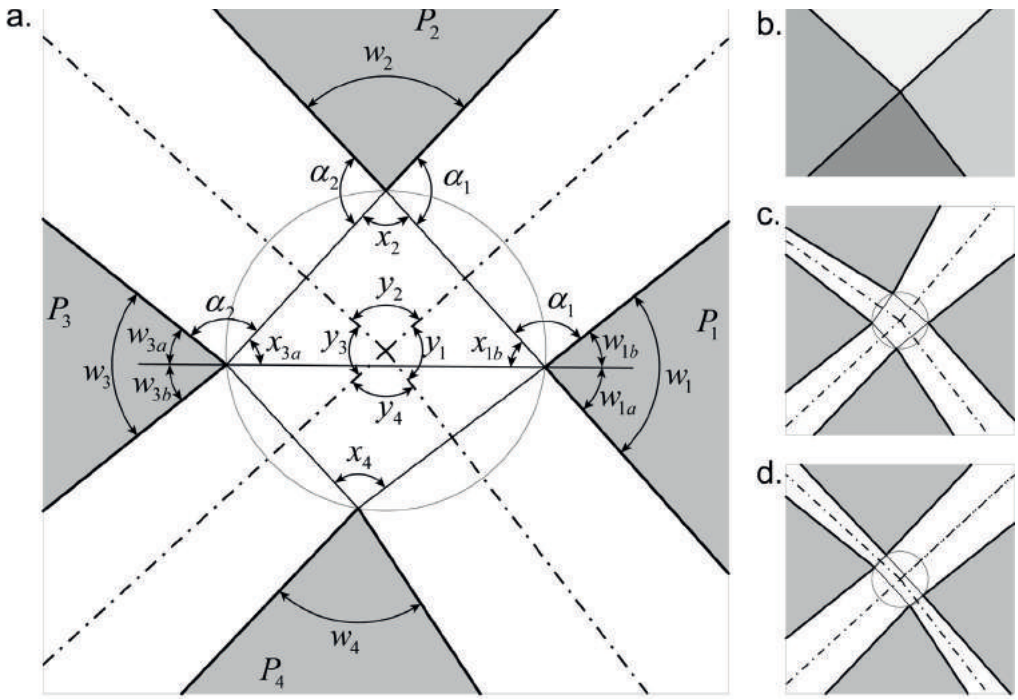

Figure 6: Different flattened states of a node from a conical mesh. The shell state is shown in b, the a, c and d display the flattened states in different configurations. The dash-dotted lines indicate the symmetric axes of the trapezoids. These axes intersect at the center of the circumcircle of the quadrilateral formed by the vertices.

the vertex of P_2, it can be derived that $w_2+\alpha_1+\alpha_2+x_2=2\pi$. By the straight angles around the vertices of P_1 and P_3, it can be formulated as $w_{1b}+\alpha_1+x_{1b}=\pi$ and $w_{3a}+\alpha_2+x_{3a}=\pi$. While the triangle between these vertices implies that: $x_{1b}+x_2+x_{3a}=\pi$. With these equations, the variable angles (i.e. α_1, α_2) can be eliminated. Then the following equation is derived: $w_2-w_{1b}-w_{3a}+2x_2=\pi$. In an alternative format, it can be expressed as: $x_2=\pi/2+(w_{1b}-w_2+w_{3a})/2$. This equation implies that the vertices of the P_2 must locate on the arc between P_1 and P_3, no matter what degrees the angles α_1 and α_2 have.

The second part of the proving explains that the arcs of the vertices of P_2 and P_4 complete a circle. Given: $x_4=\pi/2+(w_{1a}-w_4+w_{3b})/2$. Therefore, the summation of the opposite angles in the quadrilateral can be expressed as it follows:

$$x_2+x_4=\pi+\frac{w_1-w_2+w_3-w_4}{2} \tag{2}$$

Considering the node is originated from a conical mesh, which means that the angles of the four panels should meet the condition (Liu et al., 2006):

$$w_1+w_3-w_2-w_4=0 \tag{3}$$

Therefore, Equation 2 can be updated as:

$$x_2+x_4=\pi \tag{4}$$

Equation (4) implies the arc for P_2 and the arc for P_4 complete a full circle. This feature constrains the quadrilateral to be cyclic.

Since the quadrilateral is cyclic, the symmetric axes of the trapezoids intersect at the center of the circumcircle. The angles between the symmetric axes (e.g., y_1 in **Fig. 6**) meet a condition similar to conical mesh: $y_1+y_3-y_2-y_4=0$. It can be derived from $y_2=\pi-x_2$ and $y_4=\pi-x_4$. Therefore, $y_2+y_4=2\pi-x_2-x_4$. Similarly, $y_1+y_3=2\pi-x_1-x_3$. Since $x_2+x_4=\pi$, and $x_1+x_3=\pi$, it can be concluded that:

$$y_1+y_3-y_2-y_4=0 \tag{5}$$

Equation (4) is similar to the condition displayed in Equation (3).

As it is shown in dash-dotted lines in Figure 7, the symmetric axes of the trapezoids surrounding a panel form a polygon. The polygons can be seen as the extensions of the panels. In the three-dimensional conical mesh all the nodes surround by four angles meet Equation (3), and the same condition makes the extended flattened polygons in the two-dimensional configuration hold the condition of Equation (5).

These identified features help the development of further algorithmic design methods. A preliminary result of unrolling of a free-form conical mesh is displayed in Figure 7.

4. Results, reflection, and future exploration

Following the discussion on mechanical and geometrical features of the bi-stable joint, panelization, and flattening, this section describes the validation of the proposed methods through physical prototyping. The prototypes were produced using fused filament 3D printing with polylactic acid (PLA). The hinge between connectors and panels are fabricated as compliant hinges. Although the bi-stable mechanism does not have to be manufactured with compliant hinges, it is one of the most convenient methods to combine the hinge mechanism with additive fabrication. Currently, the detail design scheme for the compliant hinge is under further investigation. Some of the results demonstrate that the 3D-printing of compliant hinges is a promising design to production method for prototyping. Figure 8 shows one of the first set prototypes of the bi-stable mechanism applied on bending reconfiguration, while Figuer 9 displays the reconfiguration process of the 3D-printed saddle surface.

By extending the principles of the edge-based bi-stable mechanism as shown in Figure 8 and Figure 9, a node-based bi-stable mechanism can also be achieved. Figure 10 shows an ongoing exploration of designing a bi-stable auxetic flat-to-curve reconfigurable mechanism, which is achieved by applying the same design principles.

When comparing widely explored origami mechanisms, which require thin materials, the proposed mechanisms are compatible with thick materials. By introducing the tilted hinges, the thick materials can undergo flat-to-curved reconfiguration. The property of thickness-insensitiveness allows engineers to thicken any identified week part to reduce the local stresses.

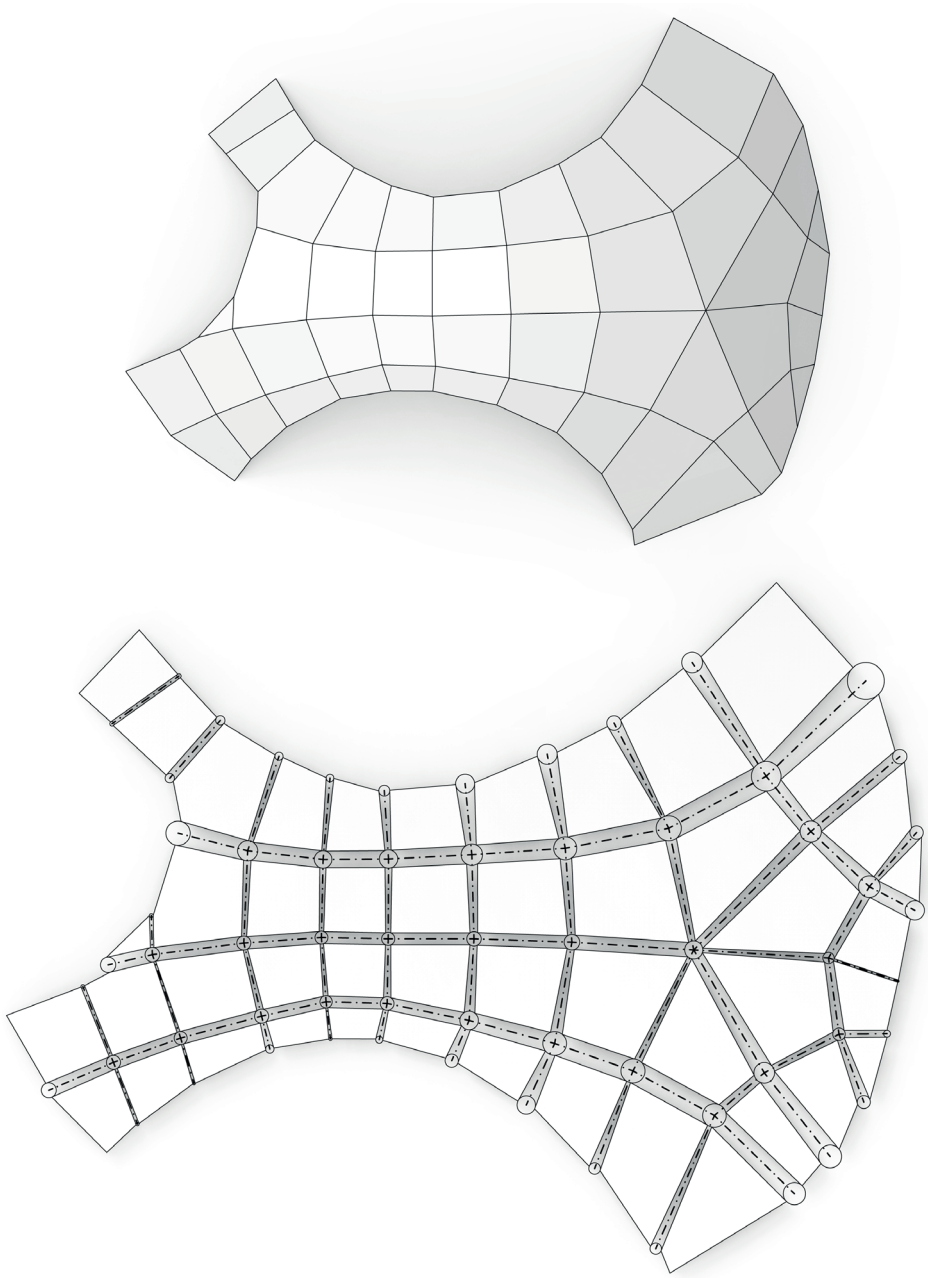

Figure 7: Top views of a free-form vault: The conical mesh (top) is translated into a flattened configuration (bottom). A node in the shell configuration will transform into a cyclic quadrilateral in the flat configuration while an edge will turn into an isosceles trapezoid. The circles in the figure denote the circumcircle of the quadrilaterals while the dash-dotted lines represent the symmetrical axes of the trapezoids.

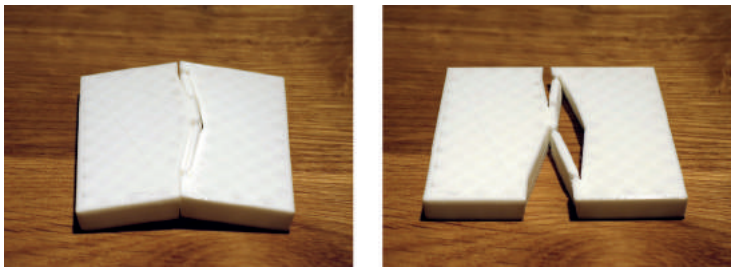

Figure 8: Test of the bi-stable joint, which is 3D printed with 5 mm thick PLA panels and 0.5 mm width compliant hinges. Pushing the panels (left), the bi-stable joint is mechanically activated and reconfigures to the curved shape (right).

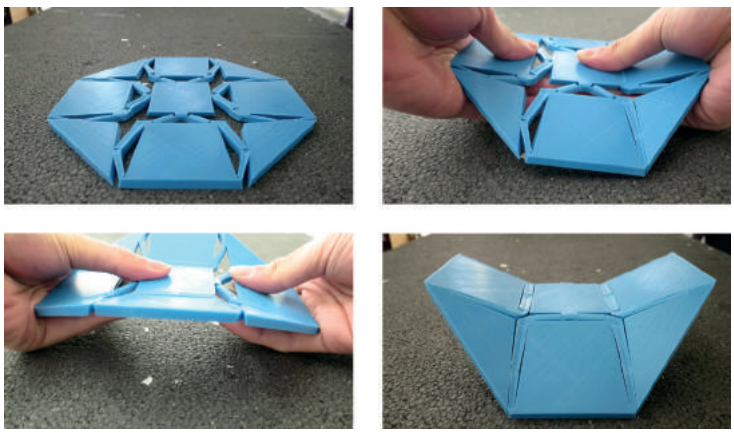

Figure 9: Reconfiguration sequences of a saddle surface produced with 3D printed PLA. It proves the concept of applying the bi-stable mechanism to a double curved shell. The sequence starts from the nine panels in the flat configuration (top left), pushing the joints one-by-one, it gradually takes the shape of the final configuration.

The exploration has identified that solution exists, under geometrical constraints and under the preliminary assumptions of zero-stiffness hinges and flexible materials. For future geometrical studies, the authors will explore and develop relevant methods to systematically translate freeform surfaces into the titled cutting patterns for the bi-stable auxetic mechanism. For the future material investigation, the authors will investigate materials to fabricate the hinges and the panels. For the structural representative prototypes, the authors will add extra weight to the scaled physical prototypes for both statical and dynamical tests to compensate scale factor.

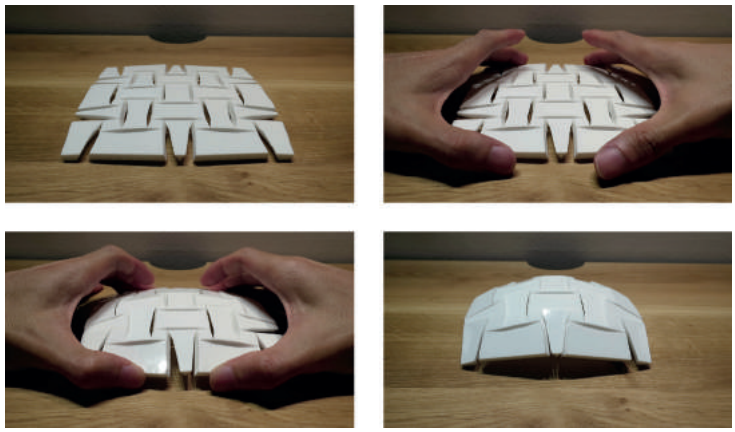

Figure 10: From flat to sphere reconfiguration with bi-stable auxetic mechanism can also be achieved with the shown design principles. By squeezing the mechanism, 25 panels connected by 16 smaller rotating node connectors are reconfigured into the pre-programed position in one step. Video of the reconfiguration can be accessed via https://youtu.be/4GcG_AurBQk.

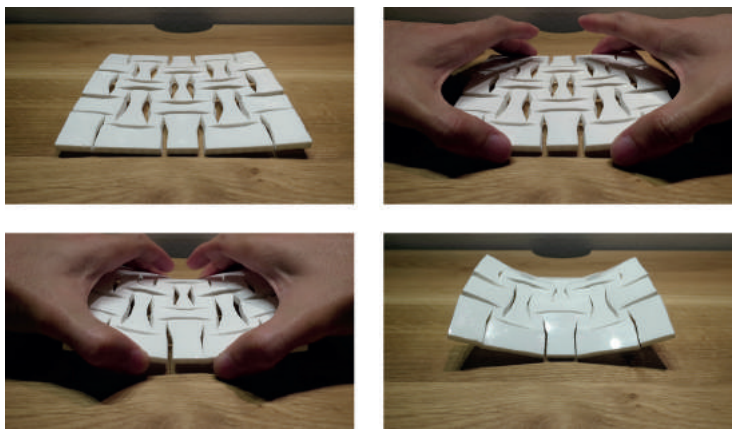

Figure 11: Flat to saddle reconfiguration with bi-stable auxetic. Same as the reconfiguration of the spherical surface, by squeezing the mechanism all the components are reconfigured into the pre-programed position in one step. Video of the reconfiguration can be access via https://youtu.be/WWHXlySTkfI.

5. Conclusion

In this research, the presented method of developing bi-stable mechanism is introduced as an approach for the assembly of shell structures.

The workflow to translate a three-dimensional curved shell structure into a flattened surface is explored, and specific geometric design constraints are discovered and proved. Validating the method, several reconfigurable shell topologies are designed and physically prototyped with bi-stable mechanisms.

In cases of any given planar quadrilateral meshes, as a necessary condition, the spaces between the edges of the flattened panels are isosceles trapezoids. While in cases that the curved surface is a conical mesh, the spaces between the flattened panels not only met the necessary condition of being isosceles trapezoid but also, as a sufficient condition, vertices of all neighboring panels are on a circle. These necessary and sufficient conditions later can be further integrated in an assembly-aware parametric modeling. The novelty of the proposed method is that it allows out-of-plane or three-dimensional reconfiguration. Consequently, the derived principles can be applied to more complex free form morphologies.

To implement the proposed reconfigurable assembly at building scales, further investigations need to address structural aspects and material properties. In macro scale design of reconfigurable shells, integrating the structural analysis in the form-finding process can inform the overall morphology of the planar mesh surfaces. In micro or material scale, further studies can address mechanical properties of the connector elements, considering fatigue for passive joints and controlled actuation for active systems. This is important as the critical force to activate the reconfiguration can be adjusted by tuning the stiffness. The strength of different bi-stable joints can be mechanically tested. The set of produced prototypes shows that in some cases the sequence of activating the bi-stable joints is important (**Fig. 9**). While in some cases as it is tested in the prototype with an auxetic property, there is no sequence and the reconfiguration happens at once (**Fig. 10** and **Fig. 11**).

Acknowledgments

The research is supported by Delft University of Technology (TU Delft) and Dessau Institute of Architecture. The first author would like to express the gratitude to Taiwanese Ministry of Education for granting the scholarship. The prototyping is sponsored by the Science Center of TU Delft.

References

Haghpanah, B., Salari-Sharif, L., Pourrajab, P., Hopkins, J., & Valdevit, L. (2016). Architected Materials: Multistable Shape-Reconfigurable Architected Materials. *Advanced Materials*. https://doi.org/10.1002/adma.201670255

Huang, N. C., & Vahidi, B. (1971). Snap-through buckling of two simple structures. *International Journal of Non-Linear Mechanics*, 6(3), 295–310. https://doi.org/10.1016/0020-7462(71)90011-4

Konakovi , M., Crane, K., Deng, B., Bouaziz, S., Piker, D., & Pauly, M. (2016). Beyond developable. *ACM Transactions on Graphics*. https://doi.org/10.1145/2897824.2925944

Liu, Y., Pottmann, H., Wallner, J., Yang, Y.-L., & Wang, W. (2006). Geometric modeling with conical meshes and developable surfaces. *ACM SIGGRAPH 2006 Papers on – SIGGRAPH '06*, 681. https://doi.org/10.1145/1179352.1141941

McKinsey Global Institute. (2017). *MGI-Reinventing-construction-A-route-to-higher-productivity-Full-report*. McKinsey & Company. Retrieved from https://www.mckinsey.com/industries/capital-projects-and-infrastructure/our-insights/reinventing-construction-through-a-productivity-revolution

Rafsanjani, A., & Pasini, D. (2016). Bistable auxetic mechanical metamaterials inspired by ancient geometric motifs. *Extreme Mechanics Letters*. https://doi.org/10.1016/j.eml.2016.09.001

Tibbits, S., McKnelly, C., Olguin, C., Dikovsky, D., & Hirsch, S. (2014). 4D PRINTING AND UNIVERSAL TRANSFORMATION. In *ACADIA 2014 Design Agency: Proceedings of the 34th Annual Conference of the Association for Computer Aided Design in Architecture* (pp. 539–548).

van Manen, T., Janbaz, S., & Zadpoor, A. A. (2017). Programming 2D/3D shape-shifting with hobbyist 3D printers. *Mater. Horiz.*, 4(6), 1064–1069. https://doi.org/10.1039/C7MH00269F

Van Mele, T., Mehrotra, A., Mendez Echenagucia, T., Frick, U., Ochsendorf, J. a., DeJong, M. J., & Block, P. (2016). Form finding and structural analysis of a freeform stone vault. *Proceedings of the IASS Annual Symposium 2016 "Spatial Structures in the 21st Century,"* 1–10.